Journal of Molecular Science

Journal of Molecular Science
Volume 35 Issue 3, Year of Publication 2025, Page 1189-1193
DoI-10.004687/1000-9035.2025.160

Journal of Molecular Science

www.jmolecularsci.com ISSN:1000-9035

Green Synthesis Of Zinc Oxide Silver Bimettalic Nano Composite From Grewia Oxyphilla Fruit Extract

M. Karthikeyan[1], R. Sureshkumar[1,*], K. Dinakaran[2,*]
[1] PG & Research Department of Chemistry, R.V.Govt. Arts College, Chengalpattu, Tamilnadu, 603001, India.
[2] Department of Chemistry, Thiruvalluvar University Vellore, Tamilnadu, 632115, India.

Article Information
Received: 12-10-2025
Revised: 28-10-2025
Accepted: 14-11-2025
Published: 26-12-2025

Keywords
Green synthesis, nanocomposite, characterization, antibacterial activity, and anti-biofilm activity.
.

ABSTRACT
The synthesis of zinc oxide silver nanocomposite by using the green synthesis method is trending now because it is economically friendly, environmentally safe, and less toxic to living organisms as well as humans and animals. There are several methods used for the synthesis of zinc oxide silver nanocomposite, like the electrochemical method, chemical reduction method, thermal decomposition method, etc., among which the green synthesis method is very much essential for the preparation of zinc oxide silver bimetallic nanocomposite. By this method of synthesis of nano composite having the multiple applications all over the field like that they are as follows medicine, catalyst, nano biosensors, power plants, fertilizer, insecticides, pesticides, herbicides, nano micro nutrients, plant growth promoters, which is used for the reduction of dye in industrial waste water treatments, food industries, etc., the synthesized zinc oxide silver bimetallic nano composite is further characterized by using the following analytical instruments they are UV-Visible absorption spectroscopy, FT-IR Spectroscopy, XRD, FESEM and EDAX spectrum. The antibacterial activity of the green synthesized zinc oxide silver bimetallic nanocomposite was performed well against gram-negative (E. coli) bacteria and gram-positive (S. aureus) bacteria, as well as the anti-biofilm activity against (E. coli) bacteria and (S. aureus) bacteria.

1. INTRODUCTION:

The green synthesis of zinc oxide silver Nanocompositeis one of the important synthesizing methods in this contemporary world. Nowadays there are several methods in the synthesis of nanocomposites; they are the electrochemical method, sonochemical method, thermal decomposition method, sol-gel method, mechanical milling method, and laser ablation method, among which the above green synthesis method is applied in the synthesis of zinc oxide silver nanocomposite.

The synthesis of zinc oxide silver nanocomposite from Grewia oxyphilla fruit extract has enhanced the stability of the formation of the nanocomposite due to the capping efficiency of the phytochemicals present in the fruit extract. The deposition of the nanocomposite is taking place due to the adjustment of the pH of the solution phase. The stability of the nanocomposite was related to different temperature parameters. There are so many advantages in this synthesis of nanocomposites, like that they are applied in the production of nanotubes, nanorods, nanofibers, nanochips in solar panels, semiconductors, quantum dots, nanofertilizers, nanopolymers, nanomedicines, etc.The Grewia oxyphylla fruit extract is much better in the preparation of nanocomposites.This plant mostly lives in tropical rain forests. Its growth differs according to the nature of the soil. This plant grows well in terracotta, mountain soil, lake areas, and stream areas.Its roots are highly stagnating the water towards the summer season. The shape of the leaves is similar to that of the beetle leaves with a strong leaf joint. It is dark in color, and its bark is

Journal of Molecular Science
Journal of Molecular Science
Volume 35 Issue 3, Year of Publication 2025, Page 1189-1193
DoI-10.004687/1000-9035.2025.160

in a brownish violet color. This plant, containing a greater number of small flowers and fruits, almost grows to about 3.5 to 4 meters in height. It has fruits that are a dark yellow color, and the seeds are part of one-third of the fruit. Its leaves are used as food for goats, its flowers produce a limited quantity of nectar, and the bees collect them in the spring season. Its fruits are used as food for squirrels, sparrows, and monkeys. It is simply called plum fruit. These leaves are mostly used for the treatment of bone fractures and inflammation of bone joints in village medicine. This plant is widely used as green fertilizer for soil in farmland. This plant grows with a group of other shrub-type plants. The synthesized zinc oxide silver bimetallic nanocompositewas stable till 350-450°C when calcinated in a muffle furnace. After calcination the purple color changed to pale brown. Further, these zinc oxide silver nanocomposites were introduced for the characterization studies by using different analytical instruments; they are UV-DRS, XRD, FT-IR, FESEM, and EDAX spectroscopic techniques. This nanocomposite sample was applied against pathogenic bacteria like gram-negative bacteria (E. coli) and gram-positive bacteria (S. aureus); thus, the concentration of synthesized zinc oxide silver bimetallic nanocomposite was about 500 µg/ml, 750 µg/ml, and 1000 µg/ml in all the wells in the test plate as well as the standard. The performance of synthesized zinc oxide silver bimetallic nanocomposite against E. coli bacteria is much better than against *S. aureus* bacteria. This was an excellent antibacterial agent when treated against such pathogenic bacteria. From the test report, the performance was determined well.Similarly, the anti-biofilm activity of the synthesized zinc oxide silver bimetallic nanocomposite against *E. coli* and *S. aureus* bacteria performed better.

2. Materials and methods

These fruits were collected from Vilangadu Forest, silver nitrate was purchased from Loba Chemicals, zinc nitrate hexahydrate was purchased from Loba Chemicals, sodium hydroxide was purchased from Merck Chemicals, double distilled water, a thermometer, pH paper, and Whatman 40 filter paper.

2.1 Preparation of fruit extract

The fruits were collected from the forest and rinsed with tap water, and they were allowed to dry for three hours. After the drying, the fruits were weighed. Only 30 grams of the fruits were taken in a well-cleaned watch glass, and the seeds were removed from the pulp. Then the pulp was smashed well by the cleaned mortar and pestle. The smashed pulp was transferred into a 300 ml beaker, and a 10% solution was prepared. It was heated for one hour to achieve 60-70°C, then it was allowed to cool till the temperature attained room temperature. Then the fruit's pulp solution was filtered using Whatman 40 filter paper. Then the filtrate was allowed to cool to 5°C by using the refrigerator.

2.2 Synthesis of zinc oxide silver nanocomposite

In the synthesis of the zinc oxide silver nanocomposite (**Fig.1**), only 30 ml of 0.01M concentration of the zinc nitrate hexahydrate solution is taken in a 200 ml beaker and 30ml of 0.01M concentration of silver nitrate solution was added into the same beaker it was allowed to agitate by using the mechanical stirrer for 15 min during agitation 30 ml of the 0.01M concentration of the fruit extract is added in drop by drop till the reaction completed after the addition of the fruit extract then 0.01M concentration of the freshly prepared sodium hydroxide solution was added till the precipitation taking place into the reaction phase and the pH of the reaction mixture is around 7.5 then it is allowed to filter and it was washed with double distilled water and it was dried at 100^0 C in oven for 24 hrs and it was collected in a morter and grinding well it is transferred into a silica crucible and heated into the muffle furnace for $350\text{-}450^0$ C for 4 hrs. The brownish violet powder was obtained; it was taken for further characterization studies.

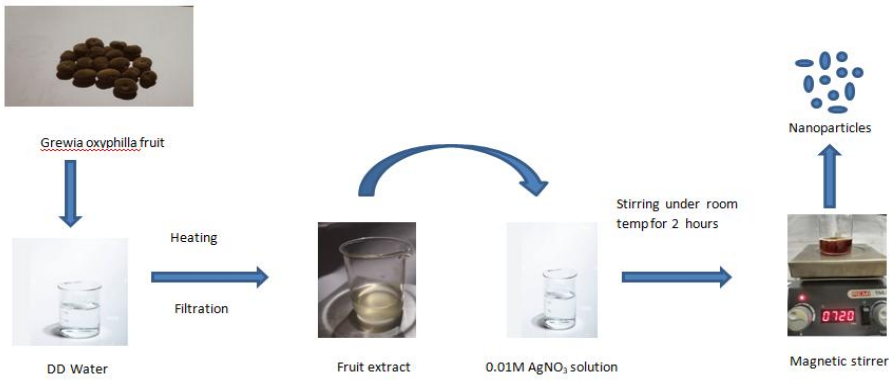

Journal of Molecular Science
Volume 35 Issue 3, Year of Publication 2025, Page 1189-1193
DoI-10.004687/1000-9035.2025.160

Fig.1 Synthetic root of metal NPs

3. RESULTS AND DISCUSSION:

3.1. UV- DRS spectroscopy:

In UV-DRS spectra, the absorption for zinc oxide nanocomposite (**Fig. 2**) will be in the range of 330 nm to 480 nm, but due to the doping with the silver nanoparticle, it is shifted to the shorter wavelength, so the peak is obtained at 267 nm, and similarly for silver nanoparticles, the peak is shifted to 397 nm.

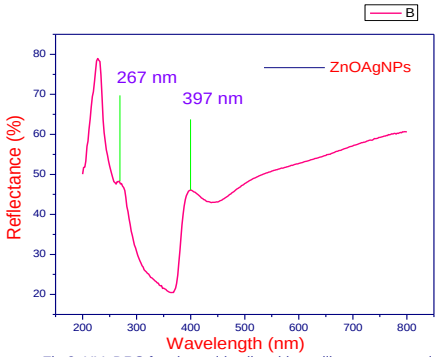

Fig.2. UV- DRS for zinc oxide silver bimetallic nanocomposite

3.2. XRD for zinc oxide silver

The synthesized zinc oxide and silver bimetallic nanoparticles showed the intense peak in x ray difractometer (**Fig.3**) in which the intensity of the peak increases with increase of the annealing temperature that is 350-450^0 C due to the effect of high temperature the particle size will increased , from the x ray diffractogram the synthesized zinc oxide silver bimetallic nanoparticles displays various lattice planes of 101, 002, 101, 111, 200, 102, 110, 103, 220, 112, 004, 202, with corresponding 2 values 32.46, 34.97,36.86, 38.75, 45.06, 48.19, 57.32, 63.61, 68.96, 69.58, 73.36 and 77.78 in this the zinc oxide component maintaining its hexagonal wurtzite syructure,while the silver adopting the FCC structure. Due to the interaction of those two components, it will result in the shifting of the peaks in the x-ray diffraction. This type of synthesized zinc oxide nanocomposite has the hexagonal wurtzite structure, among which the tetrahedral coordination is an important one to characterize this structure, in which each zinc atom is surrounded by four oxygen atoms. The diffraction peaks can shift or change due to the interaction of the zinc oxide and silver atom.

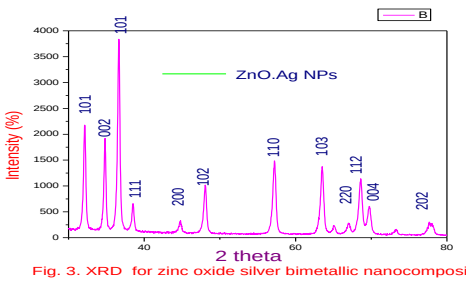

Fig. 3. XRD for zinc oxide silver bimetallic nanocomposite

3.3. FT-IR spectra for zinc oxide silver

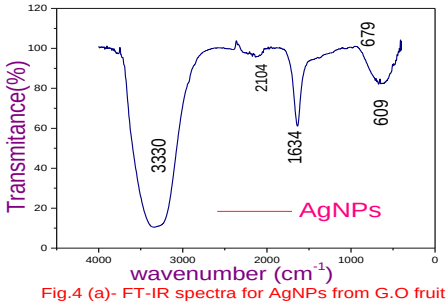

Fig.4 (a)- FT-IR spectra for AgNPs from G.O fruit extract

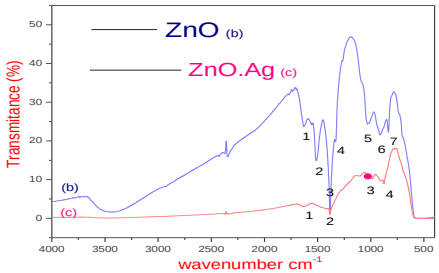

Fig. 4 (b) and (c) FT-IR spectra for ZnO and zinc oxide silver nanoparticles

The FTIR spectroscopy is a valuable one for the identification of the functional groups that may be performing the activity in the reduction of the metal or metal oxide nanoparticles (**Fig. 4(a)**) from the particular metal precursor sources, among which the zinc oxide silver bimetallic nanoparticles formed at 879 cm^{-1} and 991 cm^{-1}, the C-N group at 1103 cm^{-1}, the C=C stretching at 1625 cm^{-1}, and the C-H bending at 1410 cm^{-1}. The phenolic compound has performed its reducing and capping ability in the reduction of zinc oxide silver bimetallic nanoparticles (**Fig. 4(b)**), and because of the broad band, it appeared due to the stretching frequency of the phenolic compound at 3440 cm^{-1}.

3.4. FESEM for zinc oxide silver

This technique is an essential one for the investigation of the morphology of the synthesized silver zinc oxide nanoparticles. The scanning electron microscopic technique is an indispensable one to determine the conglomeration of the synthesized silver zinc oxide (AgZnO) bimetallic nanoparticles. From the SEM image, the structure of such a particle was identified as a hexagonal wurtzite structure, and the diameter of the particle is given as 100 nm. **Fig. 5** shows the image of the synthesized zinc oxide silver bimetallic nanoparticles.

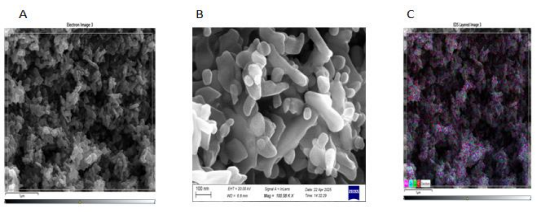

Journal of Molecular Science
Journal of Molecular Science
Volume 35 Issue 3, Year of Publication 2025, Page 1189-1193
DoI-10.004687/1000-9035.2025.160

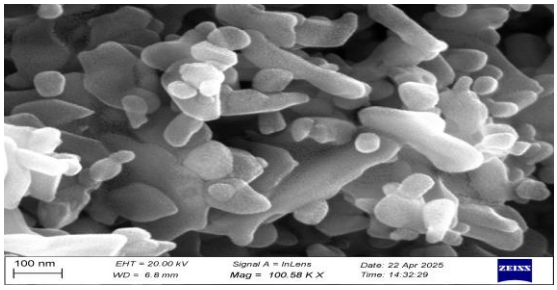

FIG. 5 .zinc oxide silver bimetallic Nanoparticles from Grewia Oxyphilla Fruit Extract

3.5. EDAX Spectrum

In elemental analysis, the other elements are C, O, and Na. The EDAX spectrum shown in **Fig.6**, shown that the zinc and silver produced the intense peak; in this, silver metal produced the minimum of 3.0 keV. Similarly, zinc metal produced 8.0 keV. Apart from that, the zinc oxide silver bimetallic nanoparticle produced about 0.5-3.0 keV.

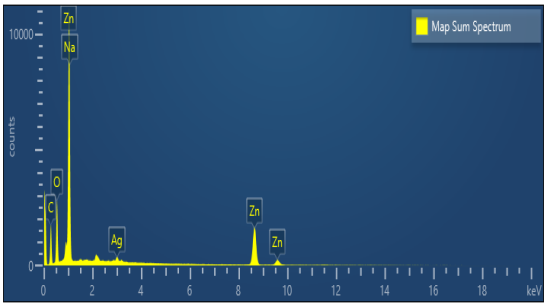

Fig.6.For EDAX spectrum

3.6. Anti bacterial activity

The antibacterial activity of green synthesized zinc oxide silver bimetallic nanocomposite against *E. coli* and *S. aureus* bacteria was good. **Table-1** displayed that the zinc oxide silver bimetallic nanocomposite was used in different concentrations, like that they are given as 500 µg/ml, 750 µg/ml, and 1000 µg/ml; the corresponding inhibition for such concentrations was 8 mm, 8 mm, and 10 mm. Similarly, the standard for such a diffusion method was ampicillin (20 µl/disc), and its inhibition was around 12 mm. From the test report, the inhibition of the synthesized zinc oxide silver bimetallic nanocomposite was almost near to the performance of the standard (ampicillin). For *E.coli* bacteria the inhibition of synthesized zinc oxide silver bimetallic nanocomposite in different concentrations is given as 500 µg/ml, 750 µg/ml, and 1000 µg/ml. The controls for such concentrations are given as 9 mm, 9 mm, and 13 mm, and the standard for the above test was ampicillin (20 µl/disc), and its inhibition was less than the performance of zinc oxide silver bimetallic nanocomposite (11 mm). From the test report, the synthesized zinc oxide silver bimetallic nanocompositeperformed well compared with the standard. So the sample was excellent for the control of *E. coli* bacteria compared to *S. aureus* bacteria. The petri plates are displayed in **Fig.7**.

Table-1 Antibacterial activity of ZnOAg against E.coli and S.aureus bacteria

Organisms	Sample (µg/ml)			Standard
	1000	750	500	
Staphylococcus aureus	10	8	8	12
Escherichia coli	13	9	9	11

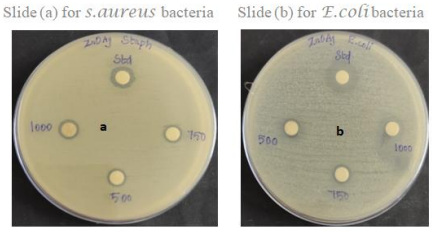

Fig.7. Zone of inhibition (mm)for pathogenic bacteria

4. CONCLUSION:

The above method of synthesizing zinc oxide silver bimetallic nanocomposite was a facile one environmentally and economically; then the zinc nitrate hexahydrate and silver nitrate were reduced in Grewia oxyphilla fruit extract. This fruit extract performed as both a reducing and capping agent due to the effect of phenolic compounds as rich phytochemicals, like that of the synthesized zinc oxide silver bimetallic nanocomposite, which was further characterized by several analytical instruments. These instruments performed well, and the crystallinity (or shape of the crystal), the presence of functional groups in the extract, and the structure and morphology of the nanocomposite were described well. The applications of the synthesized zinc oxide silver bimetallic nanocomposite were wonderful against the pathogenic bacteria like *S. aureus* and *E. coli* bacteria in antibacterial activity. From the above information, the synthesized nanocomposite was valuable for biological applications.

Author contributions:

M. Karthikeyan: writing-original draft, visualization, validation, investigation, formal analysis, data curation;
R. Suresh kumar: Writing-review & editing, investigation; **K.Dinakaran**: writing, review & editing, resources,
All authors have read and approved the manuscript.

Data availability: the data obtained and analysed during the current study are available from the corresponding author on reasonable request.

Declaration of interest:

There are no actual or potential conflict of

Journal of Molecular Science
Volume 35 Issue 3, Year of Publication 2025, Page 1189-1193
DoI-10.004687/1000-9035.2025.160

interest,including any financial,personal or other relationships with other people or organizations.

REFRENCES:

1. Advances of chitosan-based adsorbents for sustainable removal of heavy metals and anions. *Arab. J. Chem.* **15**, 103543 (2020)
2. Hosny, M. *et al.* Biogenic synthesis, characterization, antimicrobial, antioxidant, and catalytic applications of synthesized platinum nanoparticles (PtNPs) from Polygonum salicifolium leaves. *J. Environ. Chem. Eng.* **10**, 106806 (2021).
3. Abd El-Monaem, E. M. *et al.* Sustainable adsorptive removal of antibiotic residues by chitosan composites: an insight into current developments and future recommendations. *Arab. J. Chem.* **15**, 103743 (2022).
4. Jaramillo, M. F. & Restrepo, I. Wastewater reuse in agriculture: a review about its limitations and benefits. *Sustainability* **9**, 1734 (2017)
5. Didehban, A., Zabihi, M. & Shahrouzi, J. R. Experimental studies on the catalytic behavior of alloy and core-shell supported Co-Ni bimetallic nano-catalysts for hydrogen generation by hydrolysis of sodium borohydride. *Int. J. Hydrog. Energy* **43**, 20645–20660 (2018).
6. Vengatesan, M. R., Darawsheh, I. F. F., Govindan, B., Alhseinat, E. & Banat, F. Ag-Cu bimetallic nanoparticle decorated graphene nanocomposite as an effective anode material for hybrid capacitive deionization (HCDI) system. *Electrochim. Acta* **297**, 1052–1062 (2019).
7. Khan, S. A., Shahid, S. & Lee, C.-S. Green synthesis of gold and silver nanoparticles using leaf extract of clerodendrum inerme; characterization, antimicrobial, and antioxidant activities. *Biomolecules* **10**, 835 (2020).
8. Loan, T. T. & Long, N. N. Photoluminescence properties of Co-doped ZnO nanorods synthesized by hydrothermal method. *J. Phys. D Appl. Phys.* **42**, 065412 (2009).
9. Khalaj, M., Kamali, M., Costa, M. E. V. & Capela, I. Green synthesis of nanomaterials-A scientometric assessment. *J. Clean. Prod.* **267**, 122036 (2020).
10. Hosny, M., Fawzy, M., Abdelfatah, A. M., Fawzy, E. E. & Eltaweil, A. S. Comparative study on the potentialities of two halophytic species in the green synthesis of gold nanoparticles and their anticancer, antioxidant and catalytic efficiencies. *Adv. Powder Technol.* **32**, 3220–3233 (2021).
11. Omer, A. M. *et al.* Fabrication of easy separable and reusable MIL-125 (Ti)/MIL-53 (Fe) binary MOF/CNT/Alginate composite microbeads for tetracycline removal from water bodies. *Sci. Rep.* **11**, 1–14 (2021).
12. Cao, J. *et al.* Degradation of tetracycline by peroxymonosulfate activated with zero-valent iron: performance, intermediates, toxicity and mechanism. *Chem. Eng. J.* **364**, 45–56 (2019).
13. Chen, Y. *et al.* High-throughput profiling of antibiotic resistance gene dynamic in a drinking water river-reservoir system. *Water Res.* **149**, 179–189 (2019).
14. Shaltout, K. & El-Sheikh, M. Vegetation-environment relations along water courses in the Nile Delta region. *J. Veg. Sci.* **4**, 567–570 (1993).
15. International Union for Conservation of Nature, International Union for Conservation of Nature, Natural Resources. *IUCN Red List categories and criteria*.
16. Saedi, S., Shokri, M., Kim, J. T. & Shin, G. H. Semi-transparent regenerated cellulose/ZnONP nanocomposite film as a potential antimicrobial food packaging material. *J. Food Eng.* **307**, 110665 (2021).
17. Gurgur, E., Oluyamo, S., Adetuyi, A., Omotunde, O. & Okoronkwo, A. Green synthesis of zinc oxide nanoparticles and zinc oxide–silver, zinc oxide–copper nanocomposites using Bridelia ferruginea as biotemplate. *SN Applied Sciences* **2**, 1–12 (2020).
18. Cheraghcheshm, F. & Javanbakht, V. Surface modification of brick by zinc oxide and silver nanoparticles to improve performance properties. *J. Build. Eng.* **34**, 101933 (2021).
19. Yu, F. *et al.* ZnO/biochar nanocomposites via solvent free ball milling for enhanced adsorption and photocatalytic degradation of methylene blue. *J. Hazard. Mater.* **415**, 125511 (2021).
20. Ma, B. *et al.* Construction of silver nanoparticles anchored in carbonized bacterial cellulose with enhanced antibacterial properties. *Colloids Surf. A* **611**, 125845 (2021).
21. Yao, X. *et al.* Magnetic activated biochar nanocomposites derived from wakame and its application in methylene blue adsorption. *Biores. Technol.* **302**, 122842 (2020).
22. Ravikumar, S. *et al.* Costus speciosus koen leaf extract assisted cs-znx (X= O or S) nanomaterials: synthesis, characterization and photocatalytic degradation of rr 120 dye under uv and direct sunlight. *J. Mol. Struct.* **1225**, 129176 (2021).
23. Ravikumar, S. *et al.* Ag-TiO2@ Pd/C nanocomposites for efficient degradation of Reactive Red 120 dye and ofloxacin antibiotic under UV and solar light and its antimicrobial activity. *J. Environ. Chem. Eng.* **9**, 106657 (2021).
24. Dubey, R. K., Shukla, S., and Hussain, Z. (2023). Green synthesis of silver nanoparticles; A sustainable approach with diverse applications. *Chin. J. Appl. Physiology* 39, e20230007. doi:10.62958/j.cjap.2023.007
25. Durán, N., Marcato, P. D., Alves, O. L., De Souza, G. I., and Esposito, E. (2005). Mechanistic aspects of biosynthesis of silver nanoparticles by several Fusarium oxysporum strains. *J. nanobiotechnology* 3, 8–7. doi:10.1186/1477-3155-3-8
26. Dutra-Correa, M., Leite, A., De Cara, S., Diniz, I. M. A., Marques, M. M., Suffredini, I. B., et al. (2018). Antibacterial effects and cytotoxicity of an adhesive containing low concentration of silver nanoparticles. *J. Dent.* 77, 66–71. doi:10.1016/j.jdent.2018.07.010
27. Hassan, T. a.I., and Abu-Resha, R. A. (2022). Evaluation of *quorum* sening lasr and lasa genes in pseudomonus aeruginosa and ItS relation with biofilm formation. *J. Posit. Sch. Psychol.* 6 (8), 3425–3436.
28. Hosseini, M., Shapouri Moghaddam, A., Derakhshan, S., Hashemipour, S. M. A., Hadadi-Fishani, M., Pirouzi, A., et al. (2020). Correlation between biofilm formation and antibiotic resistance in MRSA and MSSA isolated from clinical samples in Iran: a systematic review and meta-analysis. *Microb. Drug Resist.* 26 (9), 1071–1080. doi:10.1089/mdr.2020.0001
29. Le Ouay, B., and Stellacci, F. (2015). Antibacterial activity of silver nanoparticles: a surface science insight. *Nano today* 10 (3), 339–354. doi:10.1016/j.nantod.2015.04.002
30. Swolana, D., Kępa, M., Kruszniewska-Rajs, C., and Wojtyczka, R. D. (2022). Antibiofilm effect of silver nanoparticles in changing the biofilm-related gene expression of Staphylococcus epidermidis. *Int. J. Mol. Sci.* 23 (16), 9257. doi:10.3390/ijms23169257
31. Vestby, L. K., Grønseth, T., Simm, R., and Nesse, L. L. (2020). Bacterial biofilm and its role in the pathogenesis of disease. *Antibiot. (Basel)* 9 (2), 59. doi:10.3390/antibiotics9020059
32. Xu, J., Li, Y., Wang, H., Zhu, M., Feng, W., and Liang, G. (2021). Enhanced antibacterial and anti-biofilm activities of antimicrobial peptides modified silver nanoparticles. *Int. J. Nanomedicine* 16, 4831–4846. doi:10.2147/ijn.s315839